Published in final edited form as:
*Biochemistry*. 2007 January 16; 46(2): 387–397. doi:10.1021/bi061642n.

# Resolving the Fluorescence Response of *E. coli* Carbamoyl Phosphate Synthetase: Mapping Intra- and Inter-Subunit Conformational Changes †

**Jason L. Johnson**[‡,*], **Joseph K. West**[‡], **Andrew D. L. Nelson**[‡], and **Gregory D. Reinhart**[§,*]
*Department of Chemistry and Physics, Southwestern Oklahoma State University, Weatherford, OK 73096, and Department of Biochemistry and Biophysics, Texas A&M University and Texas Agricultural Experiment Station, College Station, TX 77843−2128*

## Abstract

Carbamoyl phosphate synthetase (CPS) from *E. coli* is potentially overlaid with a network of allosterism, interconnecting active sites, effector binding sites, and aggregate interfaces to control its mechanisms of catalytic synchronization, regulation, and oligomerization, respectively. To characterize these conformational changes, a tryptophan-free variant of CPS was genetically engineered by substituting six native tryptophans with tyrosines. Each tryptophan was then reinserted, singly, as a specific fluorescence probe of its corresponding microenvironment. The amino acid substitutions themselves result in little apparent disruption of the protein; variants maintain catalytic and allosteric functionality, and the fluorescence properties of each tryptophan, while unique, are additive to wild-type CPS. Whereas the collective, intrinsic fluorescence response of *E. coli* CPS is largely insensitive to ligand binding, changes of the individual probes in intensity, lifetime, anisotropy, and accessibility to acrylamide quenching highlight the dynamic interplay between several protein domains, as well as between subunits. W213 within the carboxy phosphate domain, for example, exhibits an almost 40% increase in intensity upon saturation with ATP; W437 of the oligomerization domain, in contrast, is essentially silent in its fluorescence to the binding of ligands. Nucleotide and bicarbonate association within the large subunit induce fluorescence changes in both W170 and W175 of the small subunit, indicative of the type of long-range interactions purportedly synchronizing the carboxy phosphate and amidotransferase domains of the enzyme to initiate catalysis. ATP and ADP engender different fluorescence responses in most tryptophans, perhaps reflecting coordinating, conformational changes accompanying the cycling of reactants and products during catalysis.

†This work was supported by NIH grant P20 RR016478 (to JLJ) from the INBRE Program of the National Center for Research Resources at Southwestern Oklahoma State University, and by NIH grant GM33216 and Welch Foundation grant A1543 (to GDR) at Texas A&M University. Molecular graphics images were produced using the UCSF package from the Resource for Biocomputing, Visualization, and Informatics at the University of California, San Francisco, which is supported by NIH grant P41 RR-01081.

*Corresponding authors. Phone: (580) 774−3110, Fax: (580) 774−3115, E-mail: jason.johnson@swosu.edu (JLJ); or Phone: (979) 862−2263, Fax: (979) 845−4295, E-mail: gdr@tamu.edu (GDR).
‡Southwestern Oklahoma State University
§Texas A&M University

Carbamoyl phosphate synthetase (CPS)[1] from *E. coli* coordinates five substrates (2 ATP, bicarbonate, glutamine, and water) through a series reactions involving at least three unstable intermediates during the synthesis of its ultimate product, carbamoyl phosphate (1,2). Moreover, crystal structure coordinates have revealed that the reaction mechanism involves three distinct active sites separated by almost 100Å, but connected by a series of intra- and inter-molecular tunnels that presumably shuttle unstable intermediates from site to site (3-5). In the minimal mechanism of *E. coli* CPS, ATP phosphorylates bicarbonate to give rise to a carboxy phosphate intermediate within the N-terminal half (residues 1−400) of the large subunit of the $(\alpha,\beta)_1$ heterodimer; subsequently, hydrolysis of glutamine within the small subunit releases ammonia, which tunnels across subunits to react with carboxy phosphate and produce carbamate. Carbamate in turn tunnels through the protein's large subunit into the carbamoyl phosphate domain (residues 553−933), where it reacts with a second ATP to release carbamoyl phosphate.

CPS can catalyze not only its full-forward reaction (Eq 1), but also any of various partial reactions, depending upon the availability of substrates (6). For example, in the absence of nucleotides, glutamine hydrolysis (Eq 2) occurs within the amidotransferase domain of the small subunit. In the absence of an ammonia source, bicarbonate-dependent ATP hydrolysis (Eq 3) can be monitored independently within the carboxy phosphate domain of the large subunit. Finally, when supplied with the products ADP and carbamoyl phosphate, a reversal of the last step in the mechanism occurs as an ATP synthesis reaction (Eq 4). Consistent with substrate channeling, mutations of residues along the catalytic tunnels can uncouple reaction centers from each other without the concomitant disruption of these independent partial reactions (7,8). It is also revealing that a precise stoichiometry between substrates is realized in the overall reaction catalyzed by CPS; only perfect synchronization between all three active sites would prevent the wasteful accumulation and release of intermediates (9). Although the specific conformational changes that might accompany this process are unknown, it is assumed that the synchronization mechanisms are allosterically driven.

$$2\ \text{ATP}+\text{L}-\text{glutamine}+\text{HCO}_3^-+\text{H}_2\text{O} \rightarrow 2\ \text{ADP}+\text{Pi}+\text{L}-\text{glutamate}+\text{carbamoyl}-\text{P} \quad \text{Eq 1}$$

$$\text{glutamine} \rightarrow \text{glutamate}+\text{NH}_3 \quad \text{Eq 2}$$

$$\text{ATP} \xrightarrow{\text{HCO}_3^-} \text{ADP}+\text{Pi} \quad \text{Eq 3}$$

$$\text{ADP}+\text{carbamoyl}-\text{P} \rightarrow \text{ATP}+\text{CO}_2+\text{NH}_3 \quad \text{Eq 4}$$

Carbamoyl phosphate in *E. coli* condenses either with aspartate during the formation of pyrimidine nucleotides, or with ornithine during the synthesis of arginine (10,11). The allosteric effectors of *E. coli* CPS reflect the dual role of its product; UMP, in classic feedback inhibition, allosterically inhibits CPS, whereas ornithine, as a precursor, serves to activate the enzyme (12). Both act as V-type and K-type (with respect to nucleotide binding) effectors, modifying not only the full forward reaction, but also the bicarbonate-dependent $\text{ATP}_{\text{ase}}$ and, particularly, the ATP synthesis partial reactions (12-15). Competition, truncation, and labeling experiments originally suggested that UMP and ornithine bind independently within the allosteric domain at the extreme C-terminus of the large subunit (15-17); separate binding sites

[1]Abbreviations: CPS, carbamoyl phosphate synthetase; ATP, adenosine-5'-triphosphate; ADP, adenosine-5'-diphosphate; UMP, uridine-5'-monophosphate; IMP, inosine-5'-monophosphate; MOPS, 3-(N-Morpholino)propanesulfonic acid; EDTA, ethylenediaminetetraacetic acid; HEPES, 4-(2-Hydroxyethyl)piperazerine-1-ethanesulfonic acid; PEP, phospho(enol)pyruvate; AMPPNP, 5-adenylylimidodiphosphate; NATA, N-acetyltryptophanamide; 6WY, *E. coli* CPS protein genetically engineered to have all six intrinsic tryptophan substituted with tyrosine; W71, W213, W437, W461, W170, and W175 correspond to individual *E. coli* CPS proteins engineered to contain only the highlighted, native tryptophan, with the remaining five tryptophan substituted with tyrosine; CP, carbamoyl phosphate.

for the two ligands have since been verified via crystal structures (3,18). A third molecule, IMP, is competitive with UMP and was originally implicated as an allosteric activator of *E. coli* CPS (2). Later studies indicate its impact on activity is nearly negligible at 37°C; however, IMP becomes activating or inhibitory with an increase or decrease of temperature, respectively, beyond this crossover point (19).

As well as modifying the activity and affinity of CPS for substrate nucleotides, it has long been known that these same allosteric effectors also modulate the oligomerization of the protein (14,20-23). Kim and Raushel showed that oligomerization proceeds through the ordered formation of elongated $(\alpha,\beta)_2$ dimers along the allosteric domain, followed by dimer association along the oligomerization domain (residues 400−553 of the large subunit) into an $(\alpha,\beta)_4$ tetramer (24). Tetramer formation is enhanced by approximately 100–fold upon binding of either IMP or ornithine; UMP saturation, in contrast, limits the oligomerization state of CPS to the $(\alpha,\beta)_2$ dimer (24). All three ligands therefore allosterically influence the oligomerization domain from their respective binding sites over a distance of more than 50Å.

*E. coli* CPS is therefore potentially overlaid with an array of allosteric conduits of communication, controlling the synchronization of its reaction mechanism, the regulation of multiple active sites from two separate, effector binding regions, and the aggregation properties of the $(\alpha,\beta)_1$ heterodimer. Despite the extensive dynamic interplay likely existing between the protein matrix and ligand binding, little information exists on the specific nature of the conformational changes accompanying allosteric response within CPS. The resolution of multiple crystal structures have highlighted immediate residues and domains interacting directly with: Michaelis-Menten complexes of AMPPNP (26) and glutamine (26); transition-state complexes of glutamyl γ-semialdehyde (26); the products ADP and inorganic phosphate (3); as well as the allosteric effectors ornithine (3), IMP (27), and UMP (18). However, subtle long-range, allosteric conformational changes have largely escaped the resolving power of this technique. Perhaps more suited to providing insight into the solution dynamics of CPS are changes in the intrinsic fluorescence properties of the protein. The spectral properties of tryptophan, specifically, are very sensitive to localized changes in the environment of the indole moiety, and the time scale of allosteric transitions coincides well with the fluorescence lifetime of this fluorophore.

CPS from *E. coli* has six such intrinsic tryptophans. Unfortunately, the collective fluorescence response of these probes can only be interpreted as an average assessment of conformational change, and there are too many to independently resolve from each other. We report here a mutagenic approach whereby all six native tryptophans have been substituted with tyrosine and then each singly reintroduced as a specific probe of localized regions of the protein. The relative positions of each tryptophan are shown in Figure 1—note that two exist within the small subunit (W170 and W175), while the remaining four of the large subunit are distributed between the carboxy phosphate domain (W71 and W213) and the oligomerization domains (W437 and W461). With each single-tryptophan variant shown to maintain kinetic and allosteric functionality, their individual changes in steady-state intensity, fluorescence lifetime, exposure to quenching agents, and anisotropy in response to the binding of substrates and effectors provide unique information toward unraveling the potential matrix of allosteric interactions across the protein.

## Experimental Procedures

### Materials

All chemical reagents used in buffers, CPS purification, fluorescence measurements, and enzymatic assays were of analytical grade, purchased from either Aldrich, Fisher, or Sigma. Glycerol suspensions of pyruvate kinase and lactate dehydrogenase, as well as ammonium

sulfate suspensions of hexokinase and glucose-6-phosphate dehydrogenase, were purchased from Roche Applied Science. Coupling enzymes obtained in ammonium sulfate were dialyzed extensively against a buffer consisting of 50 mM MOPS-KOH, 100 mM KCl, 5 mM $MgCl_2$, and 100 mM EDTA at pH 7.0. Glucose, glutamine, ornithine, acrylamide, and the sodium salts of ADP, IMP, UMP, and PEP were all purchased from Sigma; "special quality" disodium-ATP was purchased from Roche Applied Science. Deionized distilled water was used throughout.

## Mutagenesis

The pMSO3 plasmid (28) containing *E. coli* CPS behind its natural *car*A *and car*B promoters, as well as the *E. coli* cell lines RC-50 (*car*A50, *thi*-1, *mal*A1, *xyl*-7, *rsp*L135, $\lambda^r$, $\lambda^-$, *tsx*-273) and XLI-Blue (*rec*A1, *end*A1, *gyr*A96, *thi*-1, *hsd*R17($r_k^- m_k^+$), *sup*E44, *rel*A1, $\lambda^-$, (*lac*)), were all generously provided by the lab of Frank Raushel at Texas A&M University. The pMSO3 plasmid transformed into XLI-Blue was specifically used during mutagenic protocols, whereas RC-50, lacking the gene for wild-type CPS, provided the vehicle for expressing variant CPS. The QuickChange Method of Stratagene was used to make point mutations in the CPS genes. The TGG codons for the six tryptophans were substituted, one reaction at a time, with TAC codons representing tyrosine via a scheme in which the product of one reaction served as the template for the next. The net result was a series of genes containing either one (used to express single-tryptophan variants, designated according to the sole, remaining tryptophan) or none (used to express the 6WY variant) of the original codons for tryptophan. DNA was sequenced between each reaction using the dideoxy-method with ABI "Big-Dye". Oligonucleotide synthesis and sequencing gel analyses were performed by the Gene Technologies Lab at Texas A&M University.

## CPS Purification

CPS was purified via a modification of that presented by Mareya and Raushel (29). Cells were suspended in a 100 mM phosphate buffer, pH 7.5, containing 1 mM EDTA. Following sonication, the cell extract was treated with 0.5% protamine sulfate, concentrated via an ammonium sulfate precipitation, and loaded onto a Sephacryl S-300 gel filtration column connected into an automated, AKTA-Prime chromatography system from Amersham Biosciences. Fractions were evaluated for the presence of CPS via 10% SDS-PAGE, pooled, and loaded onto a Resource-Q anion-exchange column of the AKTA-Prime system. Upon elution with a linear KCl gradient, CPS fractions were evaluated for purity on SDS-PAGE and by comparing the specific activity of the full-forward reaction to a desired value of 3.6 U/mg. Following concentration on Amicon Ultra-15 spin columns to approximately 30−40mg/mL, aliquots were frozen at −80°C for storage.

## Protein Determination

Protein determinations were made with the BCA Protein Assay Reagent (30).

## Enzymatic Assays

All kinetic experiments were performed at 25°C in a 50 mM HEPES buffer, pH 7.5, containing 100 mM KCl and 20 mM excess $MgCl_2$. ATP hydrolysis was followed via a coupling enzyme system of 20 μg/mL pyruvate kinase and 20 μg/mL lactate dehydrogenase, 1 mM PEP, 30 mM potassium bicarbonate, 0.2 mM NADH, and MgATP concentrations ranging from 0.01 − 10 mM; oxidation of NADH was monitored by a loss in absorbance at 340 nm on a Beckman-Coulter spectrophotometer equipped with 6-cell positioner. Assays of the full-forward reaction also contain 10 mM glutamine as an ammonia source, whereas this component is absent when monitoring the bicarbonate-dependent $ATP_{ase}$ partial reaction. The reverse ATP synthesis reaction was followed with a coupling enzyme system of 4 U/mL each of hexokinase and glucose-6-phosphate dehydrogenase, 10 mM glucose, 0.5 mM carbamoyl phosphate, 1 mM

NADP, and MgADP concentrations ranging from 0.005 − 10 mM; the reaction was monitored by the increase in absorbance at 340 nm accompanying the reduction of NADP. Stock solutions of carbamoyl phosphate were made freshly at least every hour. The full-forward, partial bicarbonate-dependent $ATP_{ase}$, and ATP synthesis reactions were all initiated by the addition of 10 μL of either a 0.5 mg/mL, 3 mg/mL, or 5 mg/mL CPS solution, respectively, into a 1 mL assay mix.

All non-nucleotide substrates for kinetic reactions were maintained at concentrations corresponding to saturating (> 10 X Km) for wild-type CPS, except in the case of the ATP synthesis reaction. The mechanism of substrate addition for this reverse reaction is rapid-equilibrium ordered, with ADP binding first (15); such a mechanism requires that the concentration of carbamoyl phosphate, the second substrate to bind, be adjusted to values approaching zero in order for Km values measured for ADP to correspond to true dissociation constants. Carbamoyl phosphate was therefore adjusted to 1/3 Km, i.e. 0.5 mM, in experiments monitoring ATP synthesis.

## Evaluation of Allosteric Coupling Interactions

*E. coli* CPS exhibits hyperbolic kinetics in the full-forward reaction, as well as in each of the partial reactions. The dependence of reaction rate (ν) on nucleotide substrate concentration ([A]) was therefore fit to Eq 5 below using Kaleidagraph software to evaluate values for the Michaelis-Menten constant, $K_a$, and the maximal rate of reaction, $V_{max}$:

$$\nu = \frac{V_{\max}[A]}{K_a + [A]} \qquad \text{Eq 5}$$

The coupling constants $Q_{ax}$ and $W_{ax}$ describe the total influence that an allosteric ligand "X" exerts on the binding affinity of substrate "A" and on the maximal rate of reaction, respectively, according to the following equations:

$$Q_{ax} = \frac{K_a^0}{K_a^\infty} \qquad \text{Eq 6}$$

$$W_{ax} = \frac{V_{\max}^\infty}{V_{\max}^0} \qquad \text{Eq 7}$$

where $K_a^0$ and $V_{\max}^0$ reflect rate parameters determined in the absence of an allosteric ligand, and $K_a^\infty$ and $V_{\max}^\infty$ correspond to rate parameters evaluated in the saturating presence of the allosteric ligand (31). A full, linked-function determination of $Q_{ax}$ and $W_{ax}$ involves monitoring the €dependence of each rate parameter on a broad range of concentrations of allosteric ligand to experimentally establish the limiting ratios (15,31). Here, however, given the large number of CPS variants as well the multiplicity of reaction types, values of the coupling parameters have been approximated by measuring $K_m$ and $V_{max}$ only in the absence and presence of saturating effector. Concentrations of 20 mM ornithine, 10 mM UMP, and 10 mM IMP were deemed sufficient, based on direct titrations of each ligand (described below), to occupy by >96% the corresponding binding sites of each allosteric regulator.

Binding affinities of allosteric effectors were evaluated by titrating each ligand at sub-saturating ATP concentrations and monitoring the ligand's impact on the $ATP_{ase}$ activity of CPS. The apparent dissociation constant ($K_{app}$) determined from such saturation profiles relates to the true dissociation constant of each ligand ($K_i^0$) by Eq 8 below (31):

$$K_{app} = K_i^0 \left( \frac{K_a^0 + [ATP]}{K_a^0 + Q_{ax}[ATP]} \right) \qquad \text{Eq 8}$$

The dissociation constant for ornithine ($K^0_{ix}$), for example, was determined from the increase in activity it induces upon binding to CPS; substrate concentrations were adjusted to 10 mM glutamine, 30 mM $HCO_3^-$, and 0.02 mM ATP in these assays. The concomitant decrease in $ATP_{ase}$ activity upon UMP binding was followed in the presence of 10 mM glutamine, 30 mM $HCO_3^-$, and 1 mM ATP in order to deduce its dissociation constant ($K^0_{iy}$). Finally, because IMP's direct influence on CPS activity is negligible at 25°C, its binding was followed via a competitive displacement of 5 μM UMP at 10 mM glutamine, 30 mM $HCO_3^-$, and 1 mM ATP.

In this case, Eq 9 was used to deduce IMP's dissocation constant ($K^0_{iz}$) from the measured dissociation constant, $K_{app}$, under these conditions:

$$K_{app}=K^0_{iz}\left(\frac{1+[UMP]}{K^0_{iy}}\right)\left(\frac{K^0_a+[ATP]}{K^0_a+Q_{ax}[ATP]}\right) \quad \text{Eq 9}$$

## Generation of Enzyme Ligand Forms in Fluorescence Measurements

In monitoring the impact of ligands on emission spectra, anisotropy, and acrylamide quenching, the concentration of each ligand was adjusted to at least 10 times that of its dissociation constant from native *E. coli* CPS (15). The following concentrations were used: 10mM ornithine; 0.1 mM UMP; 0.1 mM IMP; 5 mM ATP; 5 mM ADP; 10mM glutamine; 30 mM bicarbonate; and 15 mM carbamoyl phosphate.

## Steady-State Fluorescence Measurements

Ligand-induced changes in the intensity of the single-tryptophan CPS variants were made on a fluorometer equipped with a 450W xenon-arc lamp and the controller electronics of an SLM 4800 coupled with ISS PX01 photon counting electronics. The apparent emission subsequent to 300 nm excitation was collected through monochromators in the 310−410 nm range and reported as the simple integral of the emission spectrum between these limits. Although excitation was not performed at the magic angle, fluorescence anisotropy was determined separately in each case, and in all cases the changes in anisotropy are small enough so as to not significantly influence the apparent changes in intensity that are reported. Anisotropy and acrylamide quenching were monitored on a PTI QM-4 Quantamaster fluorometer equipped with a 75-watt xenon arc lamp and Glan-Thompson polarizers; 300 nm excitation and 340 nm emission through monochromators were utilized, with G-factor corrections performed for each anisotropy measurement. All fluorescence experiments were performed in 50 mM HEPES (pH=7.5), 100 mM KCl, and 20 mM excess $MgCl_2$, and corrections were made for signal contributions from the blank. When ATP and ADP additions were made, the fractional loss in intensity due to the inner filter effect was compensated for based on the intensity loss of NATA under identical experimental conditions. Protein concentrations for intensity measurements were maintained at 0.2 mg/mL; anisotropy measurements for single-tryptophan variants were performed at 1 mg/mL CPS.

To assess the relative exposure to quenching of each of the CPS tryptophan variants, steady-state intensity was monitored at 341 nm following 300 nm excitation over a 0 − 0.15 M range of acrylamide concentrations on the PTI Quantamaster described above. All protein concentrations were maintained at 0.2 mg/mL, and blank contributions were subtracted. The degree of quenching by acrylamide is reflected by the value of the Stern-Volmer constant, K, determined as the slope of the linear decrease in intensity (F°/F) with quencher concentration [Q] according to Eq 10:

$$\frac{F^0}{F}=K[Q]+1 \quad \text{Eq 10}$$

The bimolecular, collisional rate constant, $k_{sv}$, was calculated from the value of K and the lifetime of the excited state, $t^0$, as shown in Eq 11 below. Note that this equation assumes an exponential lifetime value for the fluorophore—since lifetimes here were best described using a distributional component, $\tau^0$ values used in $k_{sv}$ calculations were estimated as the center of the primary Lorentzian component modeled onto the frequency spectra of each tryptophan.

$$k_{sv}=\frac{K}{\tau^0} \quad \text{Eq 11}$$

### Dynamic Fluorescence Measurements

Frequency domain fluorometry was performed on an ISS Model K2 multi-frequency phase fluorimeter, using the 300-nm line of the "deep-UV" mode of a Spectra-Physics Model 2045 argon ion laser for excitation. Contributions from the associated 275-nm line were removed by passing the beam through a 2-mm-thick Schott WG-290 filter. Emission was collected through a Schott WG-345 long-pass cut-on filter and an emission polarizer set to the magic angle of 55° (excitation being vertically polarized). All measurements were performed with continuous stirring to minimize sample photo-bleaching, and with blank contributions subtracted (32). CPS concentrations were adjusted between 0.5−1 mg/mL for all dynamic measurements. Data analysis was performed with Globals Unlimited, obtained from the Laboratory for Fluorescence Dynamics at the University of Illinois at Urbana-Champaign.

## Results

### Kinetic & Allosteric Competency

In the genetic construction of each of the single-tryptophan variants, a gene of *E. coli* CPS was also engineered in which codons for all six intrinsic tryptophans were replaced with those of tyrosine. The resulting tryptophan-free variant, designated 6WY, represents a control against which the potential impact of the simultaneous substitutions on the kinetic and allosteric functionality of the protein can be compared. Since allosteric regulators of *E. coli* CPS primarily influence nucleotide binding, our evaluation of the allosteric competency of the tryptophan variants focused on the impact of ornithine, IMP, and UMP on the ATP- or ADP-dependent activities of the full-forward reaction and the two partial reactions, bicarbonate-dependent ATP hydrolysis and ATP synthesis.

Rate parameters for all three reactions are shown for wild-type CPS, 6WY, and each of the single-tryptophan proteins in Table 1. In the full-forward reaction, deviations in $K_m$ between wild-type CPS and 6WY are almost negligible, and the maximum rate of reaction is unaffected. Interestingly, however, increases in $K_m$ of up to 2-fold relative to wild-type are seen in the single-tryptophan variants W170, W175, W71, and W461, suggesting that conformational perturbations individually imposed by one or more tryptophan substitutions at least partially compensate for each other when appearing together. With respect to the bicarbonate-dependent $ATP_{ase}$ reaction, the tryptophan to tyrosine mutations cumulatively increase $K_m$ by approximately 1.6-fold and decreases $V_{max}$ by 1.2-fold relative to wild-type. Again, most single-tryptophan variants induce at least this much deviation relative to wild-type values, and even more so in a few cases. For example, reintroduction of W170 alone yields a protein with only one-half of the original $ATP_{ase}$ activity, whereas the W175 single-tryptophan variant binds ADP with almost 4-fold lower affinity; both correspond to tryptophan within the small subunit of the heterodimer. Conversely, the reintroduction of W213 within the carboxy phosphate domain returns the binding affinity of ADP to near normal, although activity drops to one-half that of wild-type. Finally, with respect to the rate parameters of the ATP synthesis reaction, the wild-type and 6WY enzymes are statistically indistinguishable from each other. Once again, however, single reinsertion of each small subunit tryptophan (W170 and W175) increases

$K_m$ by almost 2-fold. Distinct for this reaction, the presence of W437 perturbs $V_{max}$ more than any other single tryptophan, decreasing catalytic activity by about one-fourth.

Following the full forward reaction, the direct binding of each of the allosteric regulators was monitored via its impact on catalytic activity under sub-saturating ATP concentrations, as described under Materials and Methods. From these data, values of dissociation constants for ornithine ($K^0_{ix}$), UMP ($K^0_{iy}$), and IMP ($K^0_{iz}$) from free enzyme were determined and are shown in Table 2. Note that although differences in $K_i$ do generally exist between the tryptophan variants, the values are sufficiently similar for concentrations of 20 mM, 10 mM, and 10 mM to saturate by >92% the respective binding sites of ornithine, IMP, and UMP for all enzymes.

The total impact upon saturation that the allosteric regulators exert on nucleotide binding and catalytic activity is given by $Q_{ax}$ and $W_{ax}$, respectively (see Eq 6-7). The logarithm of the deduced coupling parameters for each tryptophan variant is portrayed graphically in Figure 2 for each reaction type; by definition, positive values of $Log(Q_{ax})$ and $Log(W_{ax})$ depict enhancement, whereas negative values reflect inhibition. Allosteric couplings associated with the full-forward reaction (Fig 2A) and the ATP synthesis reaction (Fig 2C) are nearly identical between wild-type CPS and 6WY, and only minor fluctuations exist between the single-tryptophan variants. However, with regard to the bicarbonate-dependent $ATP_{ase}$ reaction (Fig 2B), there is an approximately 3-fold increase in the UMP inhibition of the Km for ADP within 6WY relative to the native protein. The inhibition by UMP remains exaggerated in all of the single-tryptophan variants, except for W213; a reintroduction of tryptophan within this position returns the coupling to normal.

## Steady-State Emission Spectra

By exciting at the red edge of tryptophan absorbance (300nm), tryptophan is the only intrinsic residue contributing to a protein's fluorescence response, and the likelihood of energy transfer is minimized. The fluorescence emission spectrum of each of the single tryptophan variants, shown in Figure 3, therefore reflects the individualized micro-environment of the lone indole moiety remaining in each protein. Based upon an integration of each emission spectrum, W437 alone contributes almost 30% of the fluorescence signal from wild-type protein. By comparison, in decreasing order of fluorescence signal, W213, W175, W461, W71, and W170 contribute approximately 20%, 16%, 12%, 11%, and 10%, respectively. The peak wavelength, $\lambda_{max}$, and center of mass for each uncorrected emission spectrum is, respectively: wild-type, 328 nm and 340 nm; W71, 325 nm and 340 nm; W213, 329 nm and 342 nm; W437, 329 nm and 342 nm; W461, 323 nm and 336 nm; W170, 325 nm and 340 nm; and W175, 322 nm and 340 nm. The sum of the emission spectra of the single-tryptophan variants overlaps well with wild-type CPS (see Figure 3). The small discrepancy between the two spectra apparent at low emission wavelengths most likely corresponds to contributions from scattered light, which becomes multiplied six-fold when adding the single-tryptophan spectra together. The observation that the individual spectra are additive to the whole suggests that only tryptophan residues are contributing to emission and that there is no energy transfer either between tryptophan residues in the native protein or between tryptophan and tyrosine in the single-tryptophan variants, under our experimental conditions.

Saturating concentrations of the allosteric regulators ornithine, UMP, and IMP, the substrates ATP, glutamine, and bicarbonate, and the products ADP and carbamoyl phosphate were separately added to wild-type CPS and the single-tryptophan proteins to monitor for any changes in the steady-state fluorescence emission spectrum of each probe. The results are shown in Figure 4, with each panel (A-H) representing fluorescence intensity changes induced by a different ligand on each of the seven proteins. Since there are little to no ligand-induced changes in the center of mass of the spectra noted, these data are not represented. Wild-type

CPS is largely insensitive in its fluorescence response to the binding of ligands; the only notable change is an approximately 9% increase in the area of the intensity spectra upon ATP association. From these data alone, it would be unclear as to whether such a change represents a cumulative response of multiple, smaller fluorescence increases from the different tryptophans, or conversely a masked response from compensatory increases and decreases. Inspection of the changes in the single-tryptophan variants provides a clear answer: W213 exhibits a 38% increase in intensity when ATP is added, whereas W461, W170, and W175 report about 9% increases each. Only W71 and W437, representing together about 41% of the fluorescence emission of wild-type CPS, are not responsive to ATP.

Similar analyses can be made with respect to fluorescence intensity changes induced by the binding of the other ligands. ADP, in contrast to ATP, only increases the intensity of W213 and W461 by 5−6% each, induces no change in W437, W170 and W175, and decreases the intensity of W71 by about 10%. Together, these changes reflect the very small 2−4% increase of the wild-type enzyme. A comparison of the intensity changes associated with the binding of the allosteric activator ornithine, the inhibitor UMP, and IMP suggests that, of the six regions of the protein represented by the fluorescence probes, only that of W213 exhibits different responses to the three ligands. Not surprisingly, glutamine, the only ligand that binds within the small subunit, most significantly impacts the fluorescence intensity of W170 within the small subunit; however, the 9−10% and 4−5% increases by both W170 and W175 upon ATP and bicarbonate binding, respectively, as well as the 11% increase by W170 upon ADP binding, represent the most pronounced evidence from these data of allosteric communications propagated between subunits. Finally, the product carbamoyl phosphate increases the fluorescence of all the intrinsic tryptophans by 3−6%, except once again for W437. However, given the labile nature of carbamoyl phosphate, these and other fluorescence changes induced by carbamoyl phosphate addition may be equally attributable to the binding of inorganic phosphate within the various nucleotide active sites, despite the continuous use of fresh samples,.

## Tryptophan Lifetime

Fluorescence lifetimes were determined for the single-tryptophan variants in the absence and saturating presence of ligands using frequency-domain fluorometry. All data were collected with concurrent correction for contributions to the phase and modulation values associated with the solution in the absence of added protein (the blank) according to procedures previously described (32). Because the blank has a lower signal strength than the sample, the phase and modulation values obtained for the blank unavoidably have more error, which leads to a larger $X^2$ values associated with the blank-corrected values. However, since this larger error is essentially frequency-independent, it does not significantly influence the selection of an appropriate decay model to represent the behavior of the sample. The frequency dependence of phase and modulation data (raw data not shown) were fit to various models and evaluated based upon their relative $X^2$ values. Models depicting one, two, and three exponential decays, as well as a Gaussian distribution plus single exponential decay, were rejected on this basis. The model that uniformly provided the best fit for all proteins allowed for two lifetime components. The first component is represented by a Lorentzian distribution, described by the center of the distribution, $\tau 1$, the width of the distribution, w1, and the fractional contribution this component makes to the total fluorescence, f1. The second component is a single exponential decay (or discrete component) with fluorescence lifetime $\tau 2$. The results of these analyses are shown in Table 3. For every tryptophan except W71, the longer lifetime corresponds to the Lorentzian component and contributes more than 97% of the fluorescence. The very small lifetime of the discrete component, ranging from 0 − 0.27 ns sans W71, likely corresponds to scattered light. Consistent with their percent contribution to the total wild-type fluorescence emission spectra, W437 exhibits the longest lifetime, and W170 the shortest.

Although comparisons with a two-component system involving a distribution and its concomitant dimension of width can be cumbersome, here the observed changes in lifetime induced by the binding of ligands are at least qualitatively consistent with changes in the area of the intensity spectra (see Table 3). Wild-type CPS, for example, shows little lifetime or intensity change upon binding ligands, except for the ATP-induced 6% fluorescence increase; correspondingly, there is an increase in the lifetime of the Lorentzian component from 2.97 to 3.17 ns with the addition of ATP. The large 38% increase in the intensity of W213 upon ATP binding, similarly, corresponds to an increase in the fluorophore's lifetime from 2.63 to 3.60 ns. However, even in those cases where the lifetime is invariant with ligand association, specific knowledge of the excited state transition time is valuable in that it allows collisional rate constants between quenching agents and the tryptophans to be quantified, as described below.

## Acrylamide Quenching

The relative exposure of a fluorophore to collisional quenching is reflected in the Stern-Volmer constant, K, as expressed in Eq 10. The value of K is calculated directly as the slope of a plot of fluorescence intensity change vs. molar unit of quenching agent, shown in Figure 5 for the quenching by acrylamide of each of the intrinsic tryptophan of CPS. Since the value of K is directly influenced by the length of time the excited state is exposed to quenching, calculation of a true collisional rate constant, $k_{sv}$, requires normalizing against the fluorescence lifetime according to Eq 11. For example, while the slope of the Stern-Volmer plot for W437 is greater than that of W71, W461, and W175 within Figure 5, correction for the relatively longer lifetime of W437 reveals that it is actually the least exposed of the four to collision with acrylamide. Specific values of $k_{sv}$ calculated for each protein are: wild-type CPS, $1.61 \pm 0.01\ M^{-1}\ ns^{-1}$; W71, $2.19 \pm 0.03\ M^{-1}\ ns^{-1}$; W213, $2.46 \pm 0.027\ M^{-1}\ ns^{-1}$; W437 $1.31 \pm 0.02\ M^{-1}\ ns^{-1}$; W461, $1.04 \pm 0.02\ M^{-1}\ ns^{-1}$; W170, $2.35 \pm 0.05\ M^{-1}\ ns^{-1}$; and W175, $1.71 \pm 0.04\ M^{-1}\ ns^{-1}$.

Changes in the collisional rate constant induced by ligand binding reveal further insight into the conformational changes propagated across the protein matrix. Figure 6 graphically illustrates the difference between $k_{sv}$ of the ligand bound vs. unbound form of wild-type CPS and each of the single-tryptophan variants, with panels A-H separately representing each ligand. W71, positioned within the carboxy phosphate domain of the large subunit, experiences the most notable changes, oscillating between the largest increases of all tryptophan upon the binding of ornithine, UMP and ADP, and the largest decreases upon the binding of IMP and bicarbonate. Also within the carboxy phosphate domain and very close to the nucleotide active site, W213 becomes pronouncedly more protected from acrylamide quenching when CPS binds UMP, IMP, ATP, ADP, and carbamoyl phosphate. Interestingly, the $k_{sv}$ values of the two small subunit tryptophans, W170 and W175, are collectively most influenced by the association of CPS with bicarbonate ions within the carboxy phosphate domain of the large subunit.

## Anisotropy

Subsequent to excitation of a protein's tryptophan with plane polarized light, the degree of rotation of the fluorophore during the time of the excited state can be monitored in terms of the depolarization of the fluorescence emission, i.e. the anisotropy. Although the technique of time-resolved anisotropy could be used to discriminate between modes of global and local motion contributing to depolarization, here changes in the steady-state parameter are sufficient. The overall rotational motion of a protein the size of CPS is so slow relative to the fluorescence lifetime of tryptophan that differences in anisotropy will be dominated by changes in local motion experienced by the tryptophan side chain if the fluorescence lifetime and limiting anisotropy remain constant. The following steady-state anisotropy values were measured for each protein: wild-type CPS, $0.249 \pm 0.001$; W71, $0.231 \pm 0.002$; W213, $0.254 \pm 0.001$; W437, $0.282 \pm 0.001$; W461, $0.266 \pm 0.003$; W170, $0.253 \pm 0.002$; and W175, $0.189 \pm 0.002$.

As shown in Figure 7, most of the ligand-induced changes in the anisotropy values of the individual tryptophan in CPS are quite small, but are nevertheless statistically relevant. In general, ornithine and IMP increase the anisotropy of all of the intrinsic tryptophan except W437 by 0.01−0.02 units. Individually, W71 exhibits the greatest rotational response, experiencing increases of about 0.02 anisotropy units upon protein association with ornithine, IMP, and ADP. Both of the small subunit tryptophans, W170 and W175, are increased in their rotational freedom by the binding of ATP and ADP; however, bicarbonate ion imposes a degree of rigidity on the fluorophores. The least influenced by ligand binding in terms of its anisotropy is W437.

## Discussion

Despite the introduction of six amino acid substitutions across the protein, the 6WY protein appears to be free of conformational distortions that perturb function appreciably. The kinetics of the full-forward and partial reactions of 6WY and its allosteric responsiveness to ornithine, UMP, and IMP remain qualitatively intact. Moreover, the fluorescence properties of the single-tryptophan proteins, each characterized by mutation of five of the six intrinsic tryptophan into tyrosine, are additive to the total of the unaltered protein indicating no energy transfer or other spectroscopic interactions between the tryptophans. For example, the sum of the individual emission spectra (Figure 3), as well as the frequency dependence of phase and modulation (data not shown), of an equimolar mix of the proteins both overlap with those of the wild-type enzyme, with the latter providing lifetime values upon analysis comparable to native CPS ($\tau 1$ = 3.04 ns, w1 = 1.24, f1 = 0.993, and $\tau 2$ = 0 ns). Similarly, the weighted average (calculated by multiplying each by its fractional contribution to the total fluorescence emission) of the Stern-Volmer constants between acrylamide and the indole of the single-tryptophan variants provides a value of 1.76 ± 0.09, similar to the $K_{sv}$ measured for wild-type CPS of 1.61 ± 0.01. Finally, the weighted average of the anisotropy values of each single-tryptophan variant provides a value of 0.248 ± 0.006, easily within error of the anisotropy of wild-type CPS (0.249 ± 0.001).

Changes in the fluorescence parameters upon ligand binding, rather than their absolute values, are the key to tracing conformational perturbations. For example, the relatively large anisotropy and small $k_{sv}$ values of W437 suggest it is one of the more buried and restricted tryptophan residues within *E. coli* CPS; however, the lack of intensity, lifetime, quenching, and rotational response to the binding of substrates, regulators, and products characterize the region of the oligomerization domain occupied by W437 as being notably uninvolved in the potential matrix of allosteric conduits. Its particular lack of response to even those ligands which influence oligomerization (ornithine, UMP, and IMP) is notable. In contrast, W71 within the carboxy phosphate domain, but proximate to the allosteric domain, is universally most responsive to substrate and regulator binding.

The most pronounced change in any fluorescence parameter is the almost 40% increase in the fluorescence emission intensity, and concomitant 1 ns increase in lifetime, of W213 upon its association with ATP. This event is also marked by a decrease in $k_{sv}$ by over 0.6 $M^{-1}$ $ns^{-1}$ and a notable lack of anisotropy change, which in conjunction with the lifetime increase actually suggests a restriction in the motion of the fluorophore. There are two separate binding sites for ATP within CPS from which an allosteric signal might be propagated. However, W213 is positioned more than 40 Å from the nucleotide active site of the carbamoyl phosphate domain, and less than 9 Å from that of the carboxy phosphate domain. Proximity factors alone therefore implicates ATP's association within the carboxy phosphate domain as the most likely event to precipitate W213's dramatic intensity increase. The impact of the various tryptophan substitutions on the allosteric coupling parameters of CPS lends credence to this assumption. While the kinetics of the 6WY variant exhibit essentially a wild-type response to saturation by

allosteric regulators, there is one notable exception: $Q_{ay}$ between ATP and UMP for the bicarbonate-dependent $ATP_{ase}$ reaction is approximately 3-fold lower, i.e. there is a 3-fold enhanced antagonism between the two ligands. To slightly varying degrees, the coupling remains exaggerated in all of the single-tryptophan variants, except W213, which exhibits a $Q_{ay}$ value equivalent to wild-type CPS. The tryptophan to tyrosine mutation at position 213, therefore, specifically alters the ATP/UMP coupling within the carboxy phosphate domain, and not the carbamoyl phosphate domain, consistent with W213's purported fluorescence sensitivity to the carboxy phosphate domain. Interestingly, UMP itself has little impact on the fluorescence properties of W213, except for an almost 0.5 $M^{-1}$ $ns^{-1}$ decrease in $k_{sv}$.

Differences in the conformational changes induced by the regulators ornithine, UMP, and IMP can also be directly compared across the protein matrix using the six fluorescence probes. The response of the tryptophans to ornithine and IMP, both known to induce tetramerization of CPS heterodimers, are similar in most respects, except with regard to the accessibility of W71 to acrylamide quenching; ornithine increases access of the indole moiety to collision with acrylamide, whereas IMP decreases it (panels A vs. C, Figure 6). UMP and IMP, which compete for the same effector binding site, induce distinct changes in the intensity of W213 (panels B vs. C, Figure 4), the $k_{sv}$ of W71 (panel B vs. C, Figure 6), and the anisotropy of all but W437 (panels B vs C, Figure 7). Finally, ornithine and UMP, allosteric regulators with opposing influence on not only the catalytic activity but also the oligomerization of CPS, induce intra- and inter-subunit conformational changes quite distinguishable from each other via: the emission intensity of W213; the susceptibility to quenching of W71, W213, W170, and W175; and the anisotropy of W71, W213, W170, and W175 (panels A vs. B, Figures 4, 6, and 7).

Perhaps the most dramatic characteristic of *E. coli* CPS is the perfectly synchronoized function of its 3 active sites despite a separation of over 100 Å. On the basis of rapid-quench studies, the initiating event in this coordination appears to involve the formation of carboxy phosphate in the large subunit, which from a distance of approximately 40Å increases the rate of glutamine hydrolysis in the small subunit by ≈1000-fold (9). The reciprocal, however, is not true; glutamine hydrolysis only increases bicarbonate-dependent hydrolysis by a fractional amount, representing the increased rate of carboxy phosphate hydrolysis by ammonia vs. water (9). The extent to which the migration and reaction of carbamate at the final reaction center is coordinated with the first two active sites is still unknown, although these events have been identified as the probable rate-limiting steps (9). Despite these kinetic insights, little information is available relating to the putative underlying allosterism that dictates active site coordination in CPS. Changes in the fluorescence properties of select intrinsic tryptophans may here, however, reflect such synchronizing, conformational changes. For example, inter-subunit interactions are evident between the binding of substrates within the large subunit and the two probes W170 and W175 within the small subunit. When ATP binds CPS, both probes increase in intensity by 8−9% (Figure 4D), decrease in $K_{sv}$ by ≈ 0.4 $M^{-1}$ $ns^{-1}$ (Figure 6D), and increase in anisotropy by ≈ 0.01 (Figure 7D); bicarbonate ion, likewise, decreases the intensity of the two probes by 3−5% (Figure 4G), decreases their anisotropy by ≈ 0.005 (Figure 7G), and either increases (for W170) or decreases (for W175) the $K_{sv}$ by ≈ 0.3 $M^{-1}$ $ns^{-1}$ (Figure 6G). Since ATP and bicarbonate are both substrates for the formation of carboxy phosphate, the conformational changes reflected in these probes may in part parallel those accompanying the enhancement of glutamine hydrolysis during the formation of carboxy phosphate. It is also interesting with regard to these purported, inter-subunit synchronization mechanisms that ATP and ADP, while presumably binding to the same active sites, elicit quite different fluorescence responses in most of the tryptophan probes, including W170 and W175 (panels D vs. E within Figures 4, 6, and 7). It is plausible that the cycling between the tri- and di-phosphonucleotides through the carboxy phosphate active site during catalysis may in fact be part of the conformational trigger promoting glutamine hydrolysis in the small subunit, or even coordinating the carboxy and carbamoyl phosphate domains.

Tryptophan residues are not located in either the allosteric or carbamoyl phosphate domains of *E. coli* CPS. Moreover, the intrinsic fluorophores characterized here are not located within regions of the other domains specifically proposed from crystallographic or mutagenic studies to be intimately involved in allosteric transitions. Fortunately, however, the 6WY variant is now poised to serve as a template into which new, strategically positioned, tryptophan probes might be conservatively introduced. Such single-tryptophan variants are currently under design, with the intent of providing further insight into the allosteric mechanisms of synchronization, regulation, and oligomerization across *E. coli* CPS.

## Acknowledgments

We would like to thank Prof. Frank M. Raushel within the Department of Chemistry at Texas A&M University for generously providing the pMSO3 plasmid containing wild-type *E. coli* CPS, as well as the RC-50 and XLI-Blue *E. coli* cell lines for expression and genetic manipulation, respectively. We would also like to thank Jennifer Holland, Andre Marshall, and Leonard Seibold, all former undergraduate students at Southwestern Oklahoma State University, for their cursory analysis of the kinetics of the single-tryptophan variants.

## References

1. Anderson PM, Meister A. Evidence for an activated form of carbon dioxide in the reaction catalyzed by *Escherichia coli* carbamyl phosphate synthetase. Biochemistry 1965;4:2803–2809. [PubMed: 5326356]
2. Meister A. Mechanism and regulation of the glutamine-dependent carbamoyl phosphate synthetase of E. coli. Adv. Enzymol 1989;62:315–374. [PubMed: 2658488]
3. Thoden JB, Holden HM, Wesenberg G, Raushel FM, Rayment I. Structure of carbamoyl phosphate synthetase: a journey of 96Å from substrate to product. Biochemistry 1997;36:6305–6316. [PubMed: 9174345]
4. Holden HM, Thoden JB, Raushel FM. Carbamoyl phosphate synthetase: a tunnel runs through it. Current Opinion in Structural Biol 1998;8:679–685.
5. Raushel FM, Thoden JB, Reinhart GD, Holden H,M. Carbamoyl phosphate synthetase: a crooked path from substrates to products. Current Opinion in Chem. Biol 1998;2:624–632.
6. Anderson PM, Meister A. Bicarbonate-dependent cleavage of adenosine triphosphate and other reactions catalyzed by *Escherichia coli* carbamyl phosphate synthetase. Biochemistry 1966;5:3157–3163. [PubMed: 5339549]
7. Huang XY, Raushel FM. An engineered blockage within the ammonia tunnel of carbamoyl phosphate synthetase prevents the use of glutamine as a substrate but not ammonia. Biochemistry 2000;39:3240–47. [PubMed: 10727215]
8. Huang X, Raushel FM. Restricted passage of reaction intermediates through the ammonia tunnel of carbamoyl phosphate synthetase. J. Biol. Chem 2000;275:26233–40. [PubMed: 10950966]
9. Miles BW, Raushel FM. Synchronization of the three reaction centers within carbamoyl phosphate synthetase. Biochemistry 2000;39:5051–5056. [PubMed: 10819970]
10. Pierard A, Wiame JM. Regulation and mutation affecting a glutamine dependent formation of carbamyl phosphate in Escherichia coli. Biochem. Biophys. Res. Commun 1964;15:76–81. [PubMed: 5319709]
11. Robin J-P, Renverne B, Herve G. Carbamoyl phosphate biosynthesis and partition in pyrimidine and arginine pathways of Escherichia coli. In situ properties of carbamoyl-phosphate synthase, ornithine transcarbamylase and aspartate transcarbamylase in permeabilized cells. Eur. J. Biochem 1989;183:519–528. [PubMed: 2673777]
12. Anderson PM, Meister A. Control of Escherichia coli carbamyl phosphate synthetase by purine and pyrimidine nucleotides. Biochemistry 1966;5:3164–9. [PubMed: 5339550]
13. Pierard A. Control of the activity of Escherichia coli carbamoyl phosphate synthetase by antagonistic allosteric effectors. Science 1966;154:1572–1573. [PubMed: 5332549]
14. Anderson PM. Binding of allosteric effectors to carbamyl-phosphate synthetase from Escherichia coli. Biochemistry 1977;16:587–593. [PubMed: 189806]

15. Braxton BL, Mullins LS, Raushel FM, Reinhart GD. Quantifying the allosteric properties of Escherichia coli carbamyl phosphate synthetase: determination of thermodynamic linked-function parameters in an ordered kinetic mechanism. Biochemistry 1992;31:2309–2316. [PubMed: 1531767]
16. Rubio V, Cevera J, Lusty C, Bendala E, Briton H. Domain structure of the large subunit of E. coli carbamoyl phosphate synthetase: location of the binding site for the allosteric inhibitor UMP in the COOH-terminal domain. Biochemistry 1991;30:1067–1075.
17. Czerwinski RM, Mareya SM, Raushel FM. Regulatory changes in the control of carbamoyl phosphate synthetase induced by truncation and mutagenesis of the allosteric binding domain. Biochemistry 1995;34:13920–13927. [PubMed: 7577987]
18. Thoden JB, Huang X, Kim J, Raushel FM, Holden, Hazel M. Long-range allosteric transitions in carbamoyl phosphate synthetase. Protein Science 2004;13:2398–2405. [PubMed: 15322282]
19. Braxton BL, Tlapak-Simmons VL, Reinhart GD. Temperature-induced inversion of allosteric phenomena. J. Biol. Chem 1993;269:47–50. [PubMed: 8276837]
20. Trotta PP, Estis LF, Meister A, Haschemeyer RH. Self-association and allosteric properties of glutamine-dependent carbamyl phosphate synthetase. Reversible dissociation to monomeric species. J. Biol. Chem 1974;25:482–491. [PubMed: 4358554]
21. Anderson PM. Evidence that the catalytic and regulatory functions of carbamyl-phosphate synthetase from Escherichia coli are not dependent on oligomer formation. Biochemistry 1977;16:583–586. [PubMed: 189805]
22. Powers SG, Meister A, Haschemeyer RH. Linkage between self association and catalytic activity of Escherichia coli carbamyl phosphate synthetase. J. Biol. Chem 1980;25:1554–1558. [PubMed: 6243640]
23. Anderson PM. Carbamoyl-phosphate synthetase: an example of effects on enzyme properties of shifting an equilibrium between active monomer and active oligomer. Biochemistry 1986;25:5576–5582. [PubMed: 3535881]
24. Kim J, Raushel FM. Allosteric control of the oligomerization of carbamoyl phosphate synthetase from Escherichia coli. Biochemistry 2001;40:11030–11036. [PubMed: 11551199]
25. Thoden JB, Wesenberg G, Raushel FM, Holden HM. Carbamoyl phosphate synthetase: closure of the β-domain as a result of nucleotide binding. Biochemistry 1999;38:2347–2357. [PubMed: 10029528]
26. Thoden JB, Huang X, Raushel FM, Holden HM. The small subunit of carbamoyl phosphate synthetase: snapshots along the reaction pathway. Biochemistry 1999;38:16158–16166. [PubMed: 10587438]
27. Thoden JB, Raushel FM, Wesenberg G, Holden HM. The binding of inosine monophosphate to Escherichia coli carbamoyl phosphate synthetase. J. Biol. Chem 1999;274:22502–22507. [PubMed: 10428826]
28. Stapleton MA, Javid-Majd F, Harmon MF, Hanks BA, Grahmann JL, Mullins LS, Raushel FM. Role of conserved residues within the carboxyphosphate domain of carbamoyl phosphate synthetase. Biochemistry 1996;35:14352–14361. [PubMed: 8916922]
29. Mareya SM, Raushel FM. A molecular wedge for triggering the amidotransferase activity of carbamoyl phosphate synthetase. Biochemistry 1994;33:2945–50. [PubMed: 8130208]
30. Smith DK, Krohn RI, Hermanson GT, Mallia AK, Gartner FH, Provenzano MD, Fujimoto EK, Goeke NM, Olson BJ, Klenk BC. Measurement of protein using bicinchoninic acid. Anal. Biochem 1985;150:76–85. [PubMed: 3843705]
31. Reinhart, Gregory D. The determination of thermodynamic allosteric parameters of an enzyme undergoing steady-state turnover. Arch. of Biochem. and Biophys 1983;224:389–401. [PubMed: 6870263]
32. Reinhart GD, Marzola P, Jameson DM, Gratton E. A method for on-line background subtraction in frequency domain fluorometry. J. Fluorescence 1991;1:153–161.

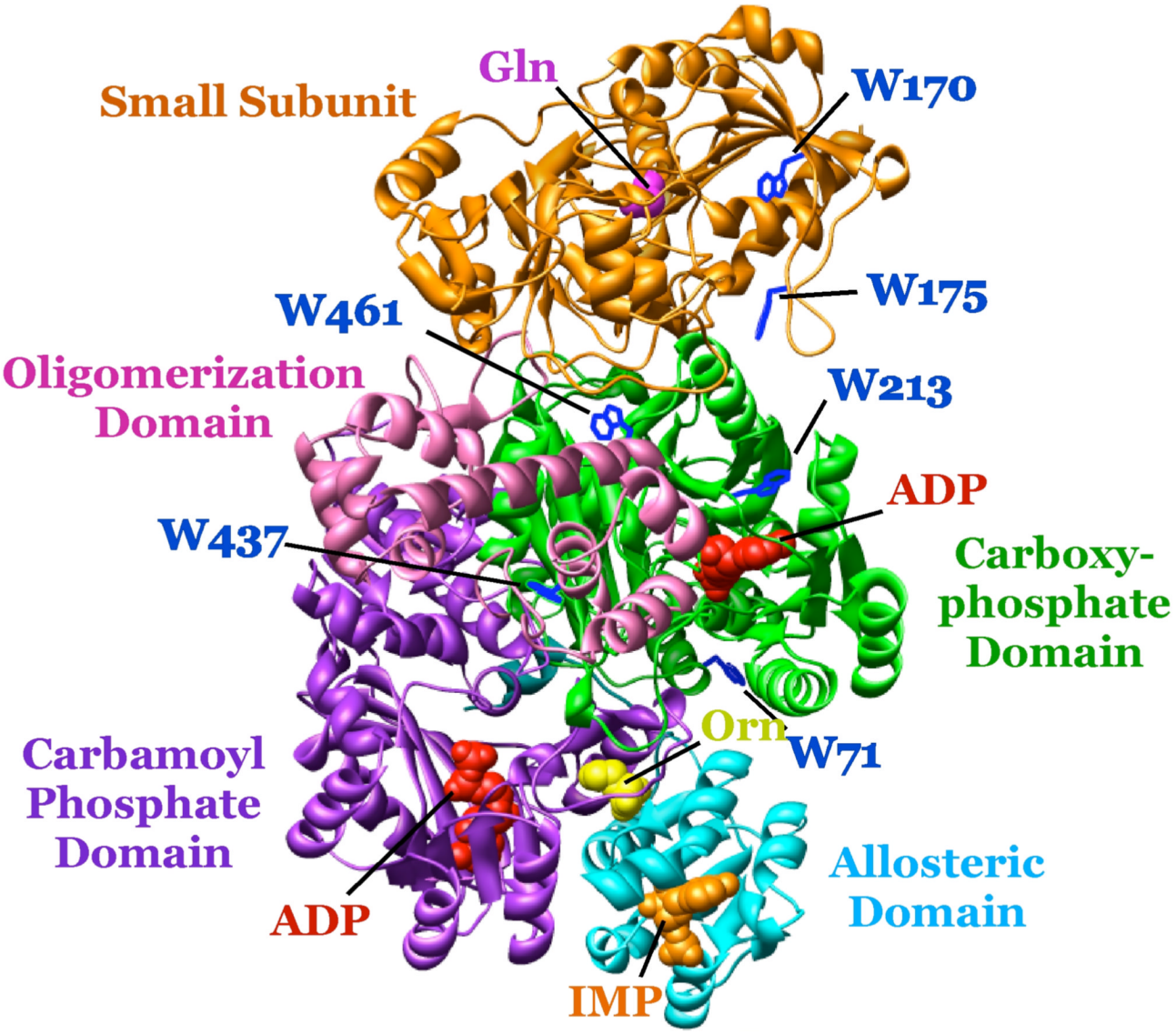


**FIGURE 1.**

Crystallographic structure of the *E. coli* CPS heterodimer emphasizing the position of the intrinsic tryptophan residues. Bound ligands include ADP (red), ornithine (yellow), and IMP (orange). Cys269, known to form a thioester adduct with glutamine at the active site of the small subunit, is shown as a magenta, space-filled residue and labeled as Gln. The six, intrinsic tryptophan residues are highlighted as dark blue, "wire" residues. Coordinates taken from 1CE8 of the PDB.

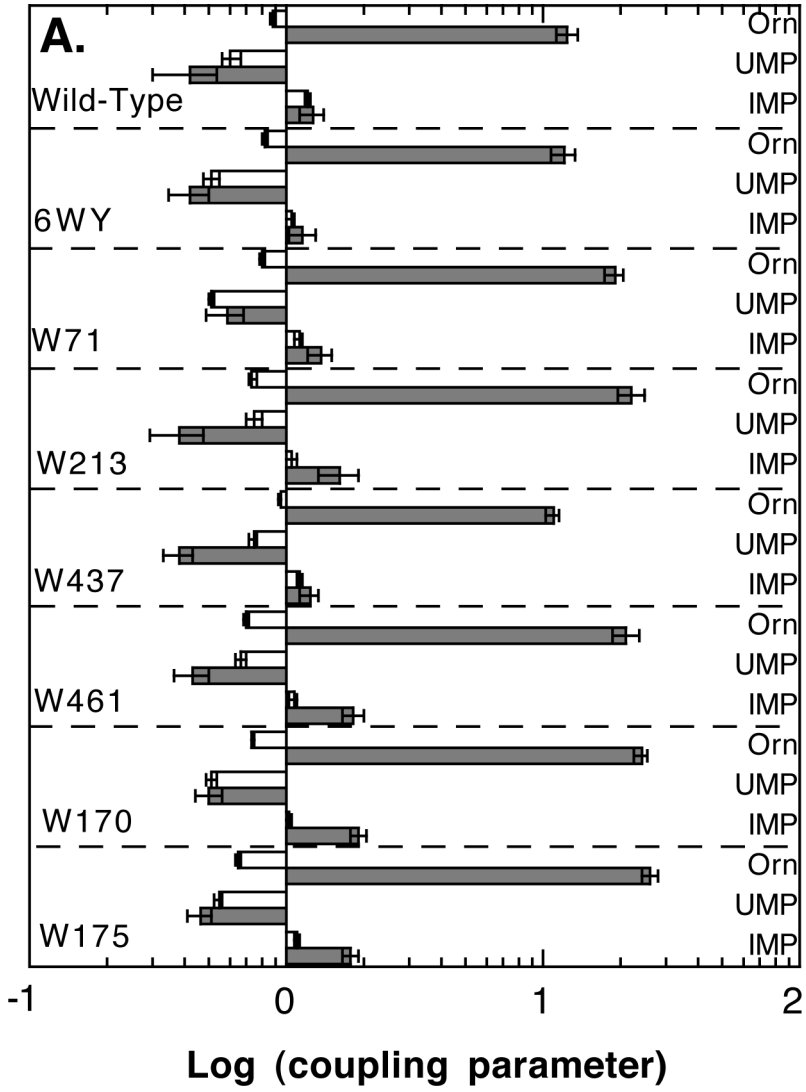

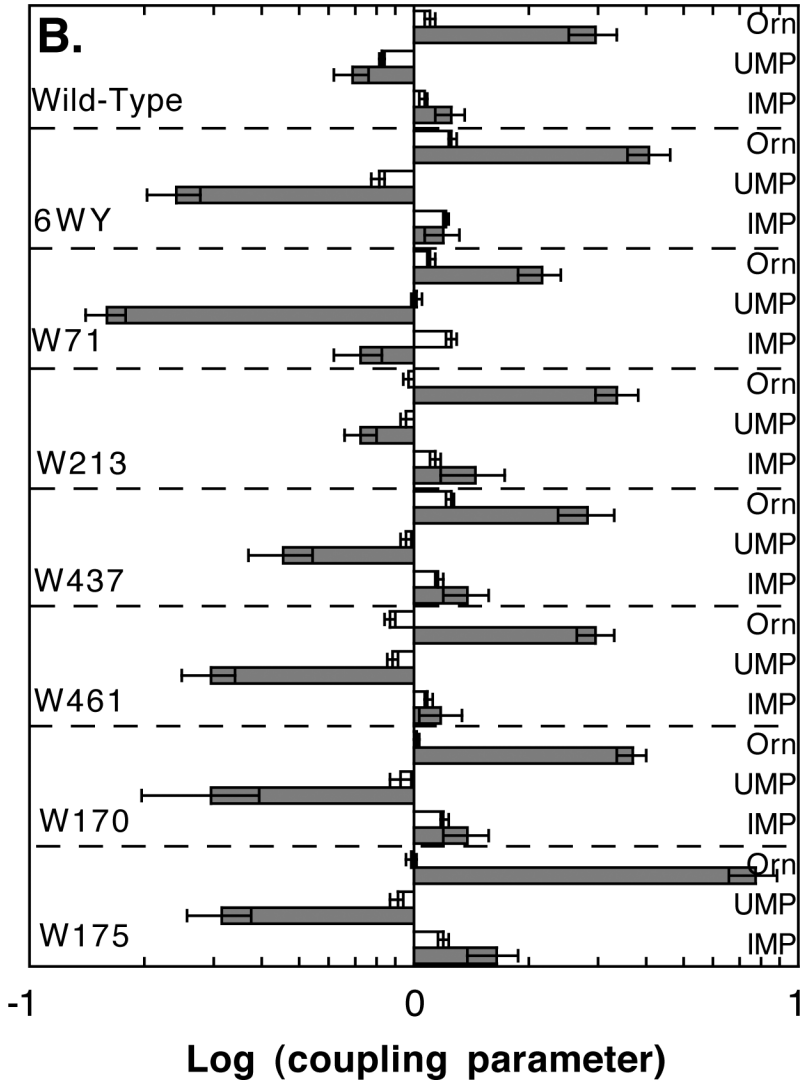

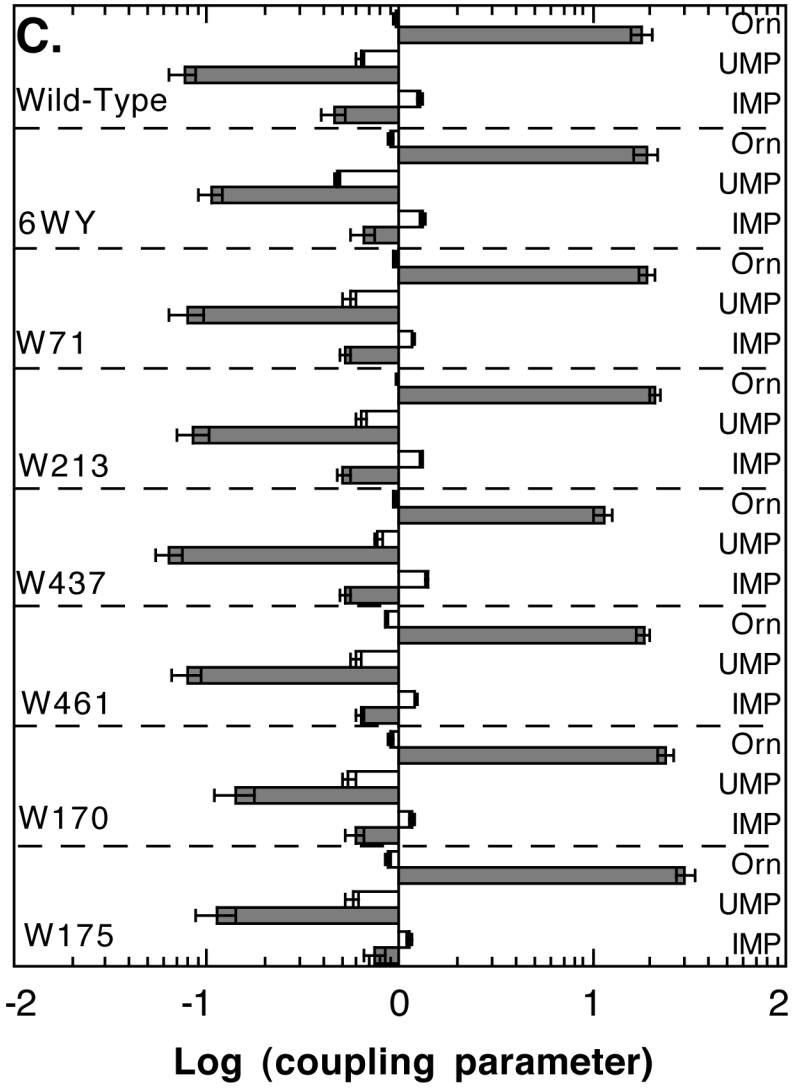


**FIGURE 2.**

Comparison of values for $Q_{ax}$ (solid bars) and $W_{ax}$ (open bars) between tryptophan variants of *E. coli* CPS. Coupling parameters were determined between substrate nucleotide and the regulators ornithine, UMP, or IMP within the (A) full forward $ATP_{ase}$ reaction, (B) bicarbonate-dependent $ATP_{ase}$ reaction, and (C) ATP synthesis reaction.

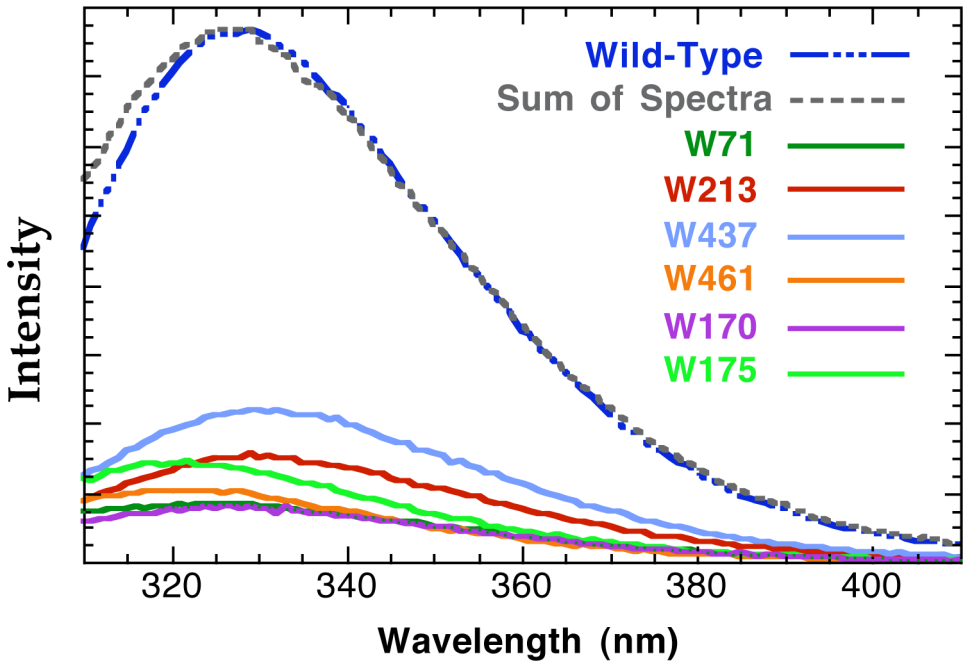


**FIGURE 3.**
Fluorescence emission spectra of wild-type *E. coli* CPS, each of the single-tryptophan variants, and an equimolar mix of the variants.

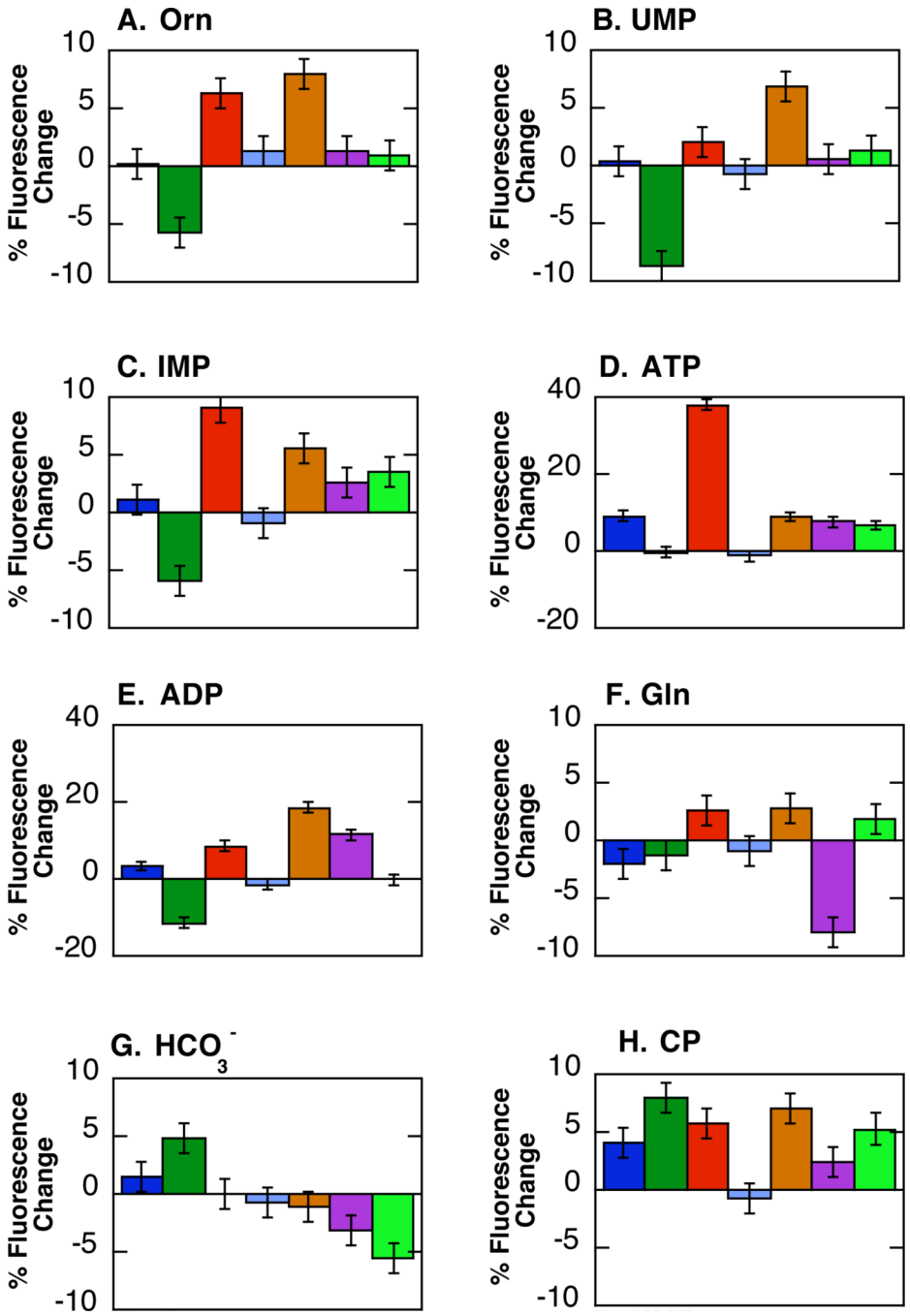


**FIGURE 4.**

Percent changes in the integrated area of the fluorescence emission spectra of wild-type *E. coli* CPS and each of the single-tryptophan variants upon saturation with (A) 10 mM ornithine, (B) 0.1 mM UMP, (C) 0.1 mM IMP, (D) 5 mM ATP, (E) 5 mM ADP, (F) 10 mM glutamine, (G) 30 mM bicarbonate, and (H) 15 mM carbamoyl phosphate. Colored bars correspond to: wild-type CPS ■, W71 ■, W213 ■, W437 ■, W461 ■, W170 ■, and W175 ■.

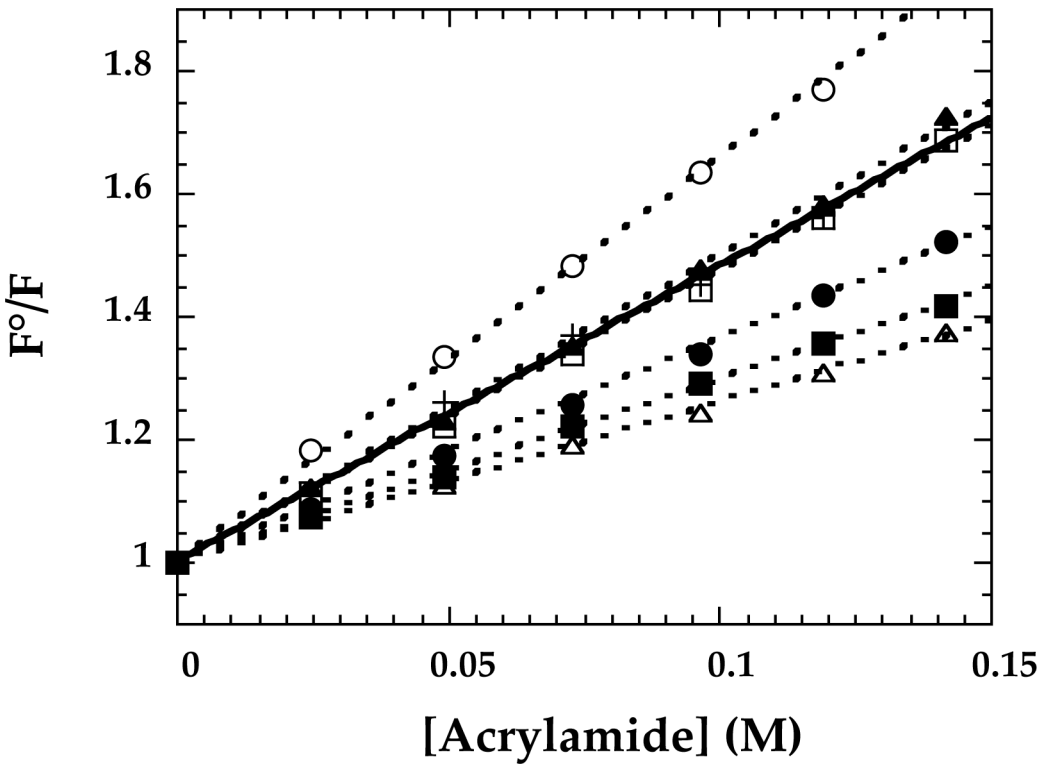


**FIGURE 5.**
Relative change in fluorescence intensity upon the addition of the quencher acrylamide for: wild-type CPS (+), W71 (△), W213 (○), W437 (□), W461 (■), W170 (▲), and W175 (•).

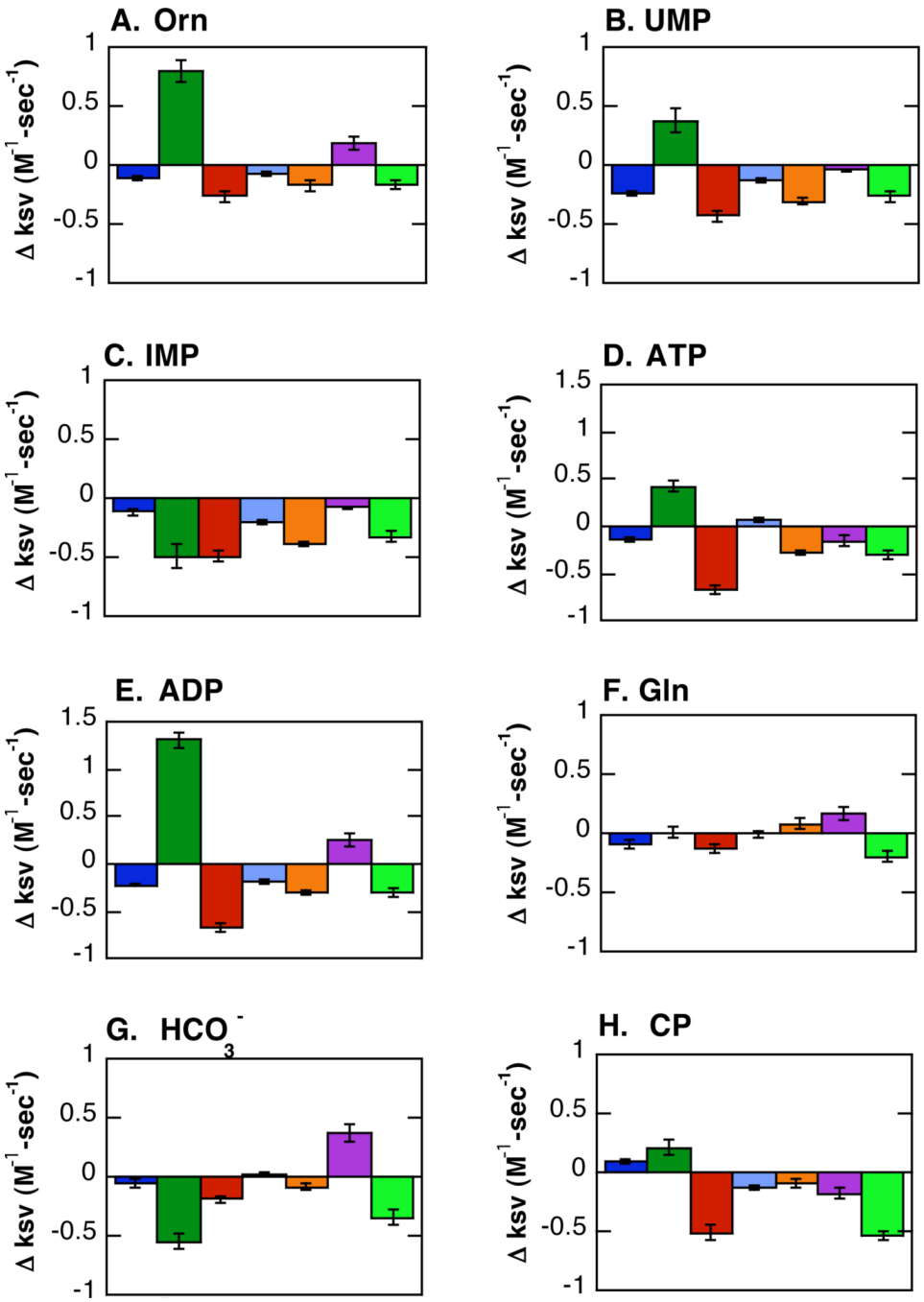


**FIGURE 6.**

Absolute changes in the collisional rate constant between acrylamide and tryptophan within wild-type *E. coli* CPS and each of the single-tryptophan variants upon saturation with (A) 10 mM ornithine, (B) 0.1 mM UMP, (C) 0.1 mM IMP, (D) 5 mM ATP, (E) 5 mM ADP, (F) 10 mM glutamine, (G) 30 mM bicarbonate, and (H) 15 mM carbamoyl phosphate. Colored bars correspond to: wild-type CPS ■, W71 ■, W213 ■, W437 ■, W461 ■, W170 ■, and W175 ■.

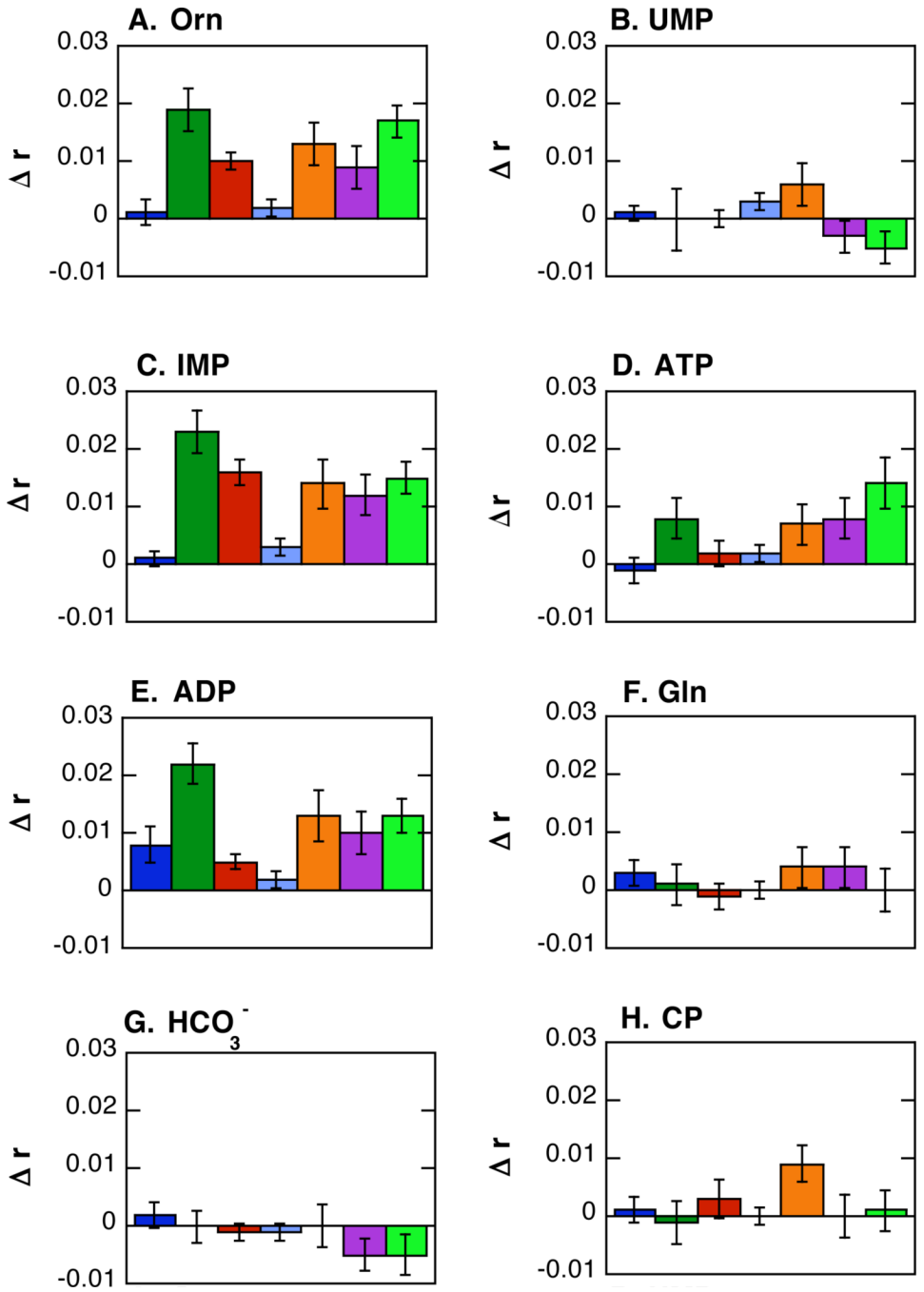


**FIGURE 7.**

Absolute changes in the anisotropy of tryptophan within wild-type *E. coli* CPS and each of the single-tryptophan variants upon saturation with (A) 10 mM ornithine, (B) 0.1 mM UMP, (C) 0.1 mM IMP, (D) 5 mM ATP, (E) 5 mM ADP, (F) 10 mM glutamine, (G) 30 mM bicarbonate, and (H) 15 mM carbamoyl phosphate. Colored bars correspond to: wild-type CPS, W71, W213, W437, W461, W170, and W175.

**Table 1**

Kinetic Parameters

| Protein | Full Forward Reaction[a] | | $HCO_3^-$ - Dependent $ATP_{ase}$[b] | | ATP Synthesis[c] | |
|---|---|---|---|---|---|---|
| | Km (mM) | Vmax (U/mg) | Km (mM) | Vmax (U/mg) | Km (mM) | Vmax (U/mg) |
| **WT** | 0.44 ± 0.04 | 2.94 ± 0.058 | 0.022 ± 0.002 | 0.420 ± 0.006 | 0.233 ± 0.024 | 0.128 ± 0.003 |
| **6WY** | 0.69 ± 0.05 | 3.08 ± 0.06 | 0.036 ± 0.003 | 0.346 ± 0.006 | 0.297 ± 0.034 | 0.131 ± 0.0036 |
| **W71** | 1.28 ± 0.09 | 3.19 ± 0.068 | 0.040 ± 0.004 | 0.285 ± 0.006 | 0.377 ± 0.024 | 0.113 ± 0.002 |
| **W213** | 0.75 ± 0.08 | 2.96 ± 0.093 | 0.026 ± 0.003 | 0.222 ± 0.005 | 0.241 ± 0.014 | 0.099 ± 0.002 |
| **W437** | 0.51 ± 0.03 | 3.04 ± 0.048 | 0.044 ± 0.005 | 0.353 ± 0.008 | 0.158 ± 0.0051 | 0.100 ± 0.001 |
| **W461** | 1.34 ± 0.10 | 3.28 ± 0.082 | 0.056 ± 0.006 | 0.394 ± 0.008 | 0.343 ± 0.0087 | 0.122 ± 0.001 |
| **W170** | 1.57 ± 0.07 | 4.63 ± 0.073 | 0.050 ± 0.003 | 0.187 ± 0.003 | 0.411 ± 0.031 | 0.106 ± 0.0020 |
| **W175** | 1.94 ± 0.08 | 4.15 ± 0.064 | 0.085 ± 0.009 | 0.224 ± 0.005 | 0.400 ± 0.034 | 0.119 ± 0.003 |

[a] Km values for ATP are shown; glutamine and bicarbonate ion concentrations were 10 mM and 30 mM, respectively.

[b] Km values for ATP are shown; bicarbonate ion concentration was 30 mM.

[c] Km values for ADP are shown; carbamoyl phosphate concentration was 0.5 mM.

**Table 2**

Dissociation Constants of Allosteric Regulators

| Protein | $K_{ix}^0$ (mM)[a] | $K_{iy}^0$ (μM)[b] | $K_{iz}^0$ (mM)[b] |
|---|---|---|---|
| **WT** | 0.83 ± 0.17 | 1.4 ± 0.4 | 0.054 ± 0.010 |
| **6WY** | 1.01 ± 0.16 | 1.8 ± 0.4 | 0.082 ± 0.019 |
| **W71** | 0.98 ± 0.15 | 2.2 ± 0.5 | 0.034 ± 0.006 |
| **W213** | 1.13 ± 0.25 | 1.5 ± 0.5 | 0.027 ± 0.007 |
| **W437** | 1.01 ± 0.14 | 1.7 ± 0.3 | 0.017 ± 0.003 |
| **W461** | 1.07 ± 0.23 | 1.7 ± 0.4 | 0.029 ± 0.005 |
| **W170** | 1.60 ± 0.28 | 2.1 ± 0.3 | 0.051 ± 0.007 |
| **W175** | 1.35 ± 0.18 | 2.0 ± 0.3 | 0.018 ± 0.004 |

[a] $K_{ix}^0$ for ornithine was determined at 10 mM glutamine, 30 mM $HCO_3^-$, and 0.02 mM ATP.

[b] $K_{iy}^0$ and $K_{iz}^0$ for IMP were determined at 10 mM glutamine, 30 mM $HCO_3^-$, and 1 mM ATP.

**Table 3**

Fluorescence Lifetime Response to Saturation by Ligands[a]

| | | No ligand | Orn | UMP | IMP | ATP | ADP | Gln | $HCO_3^-$ | CP |
|---|---|---|---|---|---|---|---|---|---|---|
| **WT** | **τ1** | 2.97 | 2.98 | 2.97 | 2.95 | 3.17 | 2.92 | 2.91 | 2.91 | 3.05 |
| | **w1** | 0.611 | 0.656 | 0.611 | 0.530 | 0.542 | 0.990 | 0.716 | 0.704 | 1.20 |
| | **f1** | 0.988 | 0.988 | 0.988 | 0.987 | 0.985 | 0.502 | 0.995 | 0.993 | 0.998 |
| | **τ2** | 0 | 0.375 | 0 | 0.192 | 0.002 | 0 | 0 | 0 | 0 |
| | **$X^2$** | 3.05 | 1.10 | 2.37 | 2.24 | 2.00 | 2.35 | 1.68 | 2.33 | 1.72 |
| **W71** | **τ1** | 1.19 | 1.05 | 1.18 | 1.07 | 1.20 | 0.910 | 1.33 | 1.34 | 1.30 |
| | **w1** | 0.858 | 0.842 | 0.819 | 1.05 | 0.925 | 0.482 | 1.58 | 1.31 | 2.08 |
| | **f1** | 0.549 | 0.506 | 0.565 | 0.545 | 0.593 | 0.483 | 0.597 | 0.607 | 0.546 |
| | **τ2** | 6.51 | 6.79 | 7.12 | 6.89 | 6.09 | 4.60 | 7.02 | 6.21 | 8.07 |
| | **$X^2$** | 7.18 | 7.66 | 7.26 | 8.02 | 6.68 | 7.08 | 7.41 | 5.05 | 2.92 |
| **W213** | **τ1** | 2.70 | 2.89 | 2.68 | 2.81 | 3.67 | 3.33 | 2.76 | 2.67 | 3.09 |
| | **w1** | 0.811 | 0.255 | 0.417 | 0.414 | 0.335 | 1.77 | 0.428 | 0.757 | 3.29 |
| | **f1** | 0.994 | 0.955 | 0.971 | 0.976 | 0.966 | 0.990 | 0.948 | 0.984 | 0.992 |
| | **τ2** | 0.116 | 0.379 | 0.205 | 0.085 | 0.163 | 0 | 0.474 | 0.008 | 0 |
| | **$X^2$** | 0.693 | 2.52 | 2.58 | 2.62 | 3.40 | 5.12 | 4.71 | 2.68 | 2.92 |
| **W437** | **τ1** | 3.60 | 3.67 | 3.71 | 3.65 | 3.50 | 3.56 | 3.75 | 3.80 | 3.86 |
| | **w1** | 0.395 | 0.148 | 0.239 | 0.286 | 0.319 | 0.005 | 0.240 | 0.403 | 1.04 |
| | **f1** | 0.984 | 0.979 | 0.982 | 0.981 | 0.975 | 0.963 | 0.981 | 0.983 | 0.982 |
| | **τ2** | 0 | 0 | 0 | 0 | 0.046 | 0.688 | 0 | 0.017 | 0 |
| | **$X^2$** | 2.76 | 3.63 | 2.69 | 4.12 | 2.74 | 5.19 | 4.19 | 3.99 | 4.94 |
| **W461** | **τ1** | 2.60 | 2.66 | 3.61 | 2.70 | 2.65 | 2.58 | 2.57 | 2.65 | 2.64 |
| | **w1** | 0.870 | 0.862 | 0.966 | 0.774 | 1.06 | 0.005 | 0.989 | 1.07 | 1.47 |
| | **f1** | 0.982 | 0.996 | 0.995 | 0.986 | 0.985 | 0.981 | 0.992 | 0.995 | 1 |
| | **τ2** | 0.264 | 0 | 0 | 0.078 | 0.259 | 0.221 | 0 | 0 | 0 |
| | **$X^2$** | 2.33 | 4.43 | 4.83 | 3.42 | 6.82 | 6.45 | 2.49 | 1.63 | 3.86 |
| **W170** | **τ1** | 2.16 | 2.26 | 2.15 | 2.13 | 3.00 | 2.10 | 2.58 | 2.11 | 3.70 |
| | **w1** | 0.156 | 0.168 | 0.359 | 0.219 | 0.005 | 0.005 | 0.159 | 0.990 | 6.66 |
| | **f1** | 0.975 | 0.943 | 0.995 | 0.992 | 0.513 | 0.988 | 0.575 | 0.209 | 0.744 |
| | **τ2** | 0.035 | 0.057 | 0 | 0 | 1.51 | 0.053 | 1.40 | 0 | 1.75 |
| | **$X^2$** | 2.08 | 5.08 | 3.76 | 5.84 | 6.04 | 8.37 | 3.52 | 2.87 | 7.54 |
| **W175** | **τ1** | 2.61 | 2.72 | 2.60 | 2.62 | 2.62 | 2.66 | 2.72 | 2.73 | 3.50 |
| | **w1** | 0.566 | 0.275 | 0.005 | 0.446 | 0.182 | 0.005 | 0.206 | 0.401 | 3.69 |
| | **f1** | 0.976 | 0.968 | 0.934 | 0.975 | 0.958 | 0.970 | 0.957 | 0.963 | 0.993 |
| | **τ2** | 0.165 | 0.047 | 0.259 | 0 | 0.412 | 0 | 0.187 | 0.132 | 0.007 |
| | **$X^2$** | 6.72 | 3.87 | 5.28 | 4.09 | 2.74 | 7.28 | 7.49 | 8.22 | 11.3 |

[a] Data were fit to a model allowing for a single Lorentzian lifetime τ1 of width w1 and fractional contribution to the total fluorescence of f1, and a second discrete lifetime τ2.